Vol. 17, No.2 April-June 2025

MULTIMODAL EVALUATION OF COLLAGEN-BASED BIOMIMETIC SCAFFOLDS ENRICHED WITH KERATIN AND HYDROXYAPATITE: INTEGRATION OF SEROLOGICAL, IMMUNOLOGICAL, AND HISTOLOGICAL ANALYSIS IN A BILATERAL OSTEOCHONDRAL RAT MODEL

Florin Popescu [1], Mădălina Albu Kaya[2], Diana-Larisa Ancuța[3*], Cristin Coman [3,4*], Florica Bărbuceanu[4,5], Vlad Vuță[4], Norin Forna[6], Adrian Barbilian[1]

[1]Department of Orthopedics and Traumatology, Faculty of Medicine, University of Medicine and Pharmacy "Carol Davila", 8 Eroii Sanitari Bvd., 050474, Bucharest, Romania
[2]National Research and Development Institute for Textiles and Leather—Division Leather and Footwear Research Institute, 93 Ion Minulescu Str., 031215, Bucharest, Romania
[3]"Cantacuzino" National Military Medical Institute for Research and Development, Splaiul Independentei 103, 050096, Bucharest, Romania
[4]University of Agronomic Sciences and Veterinary Medicine, Faculty of Veterinary Medicine, Splaiul Independentei 105, 050097, Bucharest, Romania
[5]Institute for Diagnosis and Animal Health, 63 Dr. Staicovici Str., 050557, Bucharest, Romania
[6]Faculty of Medicine, University of Medicine and Pharmacy "Grigore T.Popa", Ĭasi, Romania

*Corresponding author: Diana-Larisa Ancuța email diana.larisa.ancuta@gmail.com;
Cristin Coman email comancristin@yahoo.com;

Abstract

This study evaluates the regenerative potential of three types of collagen-based biomimetic scaffolds in osteochondral defects in Wistar rats. Formulations tested included: F1 (pure collagen - control), F5 (collagen with hydroxyapatite - for osteoconductivity assessment), and F6 (collagen with hydroxyapatite and keratin - for osteogenic and immunomodulatory potential). Using a bilateral osteochondral defect model, the research integrated serologic, immunologic, and histologic analysis over 60 days. All scaffolds showed excellent hemocompatibility (<5% hemolysis). Cytokine profiles revealed that F6 reduced the pro-inflammatory cytokines (IL-6, IL-8, TNF-α) and increased the anti-inflammatory IL-10, indicating an environment favorable for regeneration. C-reactive protein levels were decreased in the F6 group, but the serum alkaline phosphatase was significantly increased, suggesting intense osteoblastic activity. Histological evaluation confirmed the superiority of the F6 scaffold, with high scores for cell density, collagen matrix organization, mineralization, and vascularization. The results demonstrate that the addition of keratin to the collagen-hydroxyapatite composite creates a superior scaffold that modulates the systemic immune response and promotes bone regeneration.
These findings consolidate the further development of keratin-enriched biomimetic composites to act as scaffolds for regenerative strategies in orthopedic surgery.

Keywords: biomimetic scaffold, collagen, hydroxyapatite, keratin, osteochondral regeneration

Introduction

Given the complexity of their nature and the frequent delay in receiving emergency treatment, such injuries often result in long-term consequences, requiring secondary prolonged therapeutic interventions, extended follow-up, and potentially permanent functional impairment [1,2]. Even when patients make it through the initial phase and their limbs are saved, they often have to go through long healing processes, deal with chronic pain, limited mobility, and the need for multiple surgeries or regenerative therapies [3,4]. Post-traumatic and degenerative osteoskeletal pathology is becoming a bigger problem in current orthopedic

DOI : 10.62610/RJOR.2025.2.17.74

treatment, mostly because it affects the morphofunctional integrity of the osteochondral unit [5]. The growing frequency of injuries and chronic conditions affecting the articular cartilage, underlying subchondral bone, and even large parts of the entire bone itself requires novel regenerative strategies to restore structure and function [6]. Osteochondral lesions often cause pain, loss of mobility, and early osteoarthritis. Hence, it is important to use focused and fast treatment methods [7].

Hydroxyapatite (HA) is a type of calcium phosphate ceramic with a chemistry that resembles well the bone mineral content [8,9]. Composite scaffolds composed of collagen and HA are already well established in bone tissue engineering [10-12]. Collagen (COLL) is the main part of the extracellular bone matrix. It is biocompatible and provides structural support. HA, on the other hand, is a type of calcium phosphate ceramic that has a chemical structure similar to native bone mineral. It is often added to improve osteoconductivity and mechanical strength [9] Keratin (K) is a protein that hasn't been studied as much in bone regeneration, but it is well known for its ability to influence the immune system and help cells stick together, grow, and form new blood vessels [13,14]. When integrated into a collagen-composite scaffold, keratin may provide synergistic effects that facilitate both structural integrity and biological performance [15]. Keratin-based scaffolds are a new topic in tissue engineering because they help mesenchymal stem cells (MSCs) differentiate, speed up tissue repair, and create a good healing environment [16,17].

Preclinical animal studies are the next step for validating the efficacy and safety of new biomaterials. However, following the ethical imperatives of the 3Rs (Replacement, Reduction, and Refinement), such studies must be carried out with increasing rigor [18]. It is important to reduce biological variability and to maximize the scientific value of each animal used [19]. Therefore, the design of *in vivo* protocols should aim to extract multifaceted data from a single experimental cohort, integrating systemic, and histological assessments.

The Wistar rat (Rattus norvegicus) is an established animal model used in preclinical research to study osteoarticular pathologies. Its skeletal structure, rate of bone remodeling, and metabolic and immunological responses present strong analogies with human physiology, making it an excellent surrogate for studying bone repair, scaffold integration, and inflammatory modulation [20,21]. The rat experimental model accumulated good research data about its metabolic pathways and hormonal cycles that regulate bone metabolism and turnover, providing an easier and standardized way of testing biomaterials for development in orthopedic and stomatological applications [22,23]. This strain is preferred from a logistical point of view because it is easy to handle, docile, and inexpensive, which makes it easier to undertake long-term research. In osteochondral defect models, Wistar rats have shown consistent patterns of bone regeneration and vascular response comparable to those observed in larger animal models or humans, especially when evaluating biomaterials [24,25].

This study aims to investigate the regenerative behavior of three scaffold

DOI : 10.62610/RJOR.2025.2.17.74

formulations—collagen-only (COLL), collagen-hydroxyapatite (COLL-HA), and collagen-hydroxyapatite-keratin (COLL-HA-K)—implanted into a rat osteochondral defect model over 60 days.

In our research, by integrating histological, microstructural, and serological parameters, we want to underline the role of scaffold composition in guiding sensitive aspects of tissue regeneration and immune response.

As part of our initial experimental flow ideas and using the promising data obtained from the initial studies, this third study focuses on a reduced selection of biocomposites selected for in vivo testing [26]. Our goal is to thoroughly validate the regenerative properties of the composites through proven scientific methods: the hemocompatibility analysis, the spectrum of the immune response, the level of the osteogenic markers induction, and the histopathological evaluation.

After the initial experimental stages of our research, we identified the most promising biomaterials, which, in our opinion, have the best chance of regenerative potential in osteochondral applications [26]. This early work helped us reduce the research focus and better direct the next steps toward a smaller collection of scaffolds with the right in vitro and in vivo qualities.

The level of hemolytic risk for all the composite formulations was evaluated in vitro, following the current ASTM F756-00 regulations. A characteristic of an effective biocompatible material is good hemocompatibility, which comes with a low chance of erythrocyte lysis [27].

To evaluate if the materials examined will induce inflammation, the IL-6, IL-8, TNF-α, and IL-10 blood levels were measured [28,29].

The histopathological analysis highlights the augmented regenerative process induced by the presence of the biomimetic composites. Using data obtained from the quantitative scoring of cell density, matrix deposition, and vascularization, histology was part of the final integrative method of objectification that combined macroscopic slide imaging scores with the serological data.

Combining all these methodologies forms a complete algorithm for scaffold evaluation. This study exemplifies a multidisciplinary approach in line with the biomimetic philosophy of reproducing the intricate complexity of biological structures and systems through material science and regenerative engineering.

Materials and Methods

Scaffold Preparation

Three composite scaffold types were selected for the study from eight initial formulations [26,30]: F1 (pure collagen – as control), F5 (collagen with hydroxyapatite - for osteoconductivity assessment), and F6 (collagen with hydroxyapatite and keratin - for the convergent osteogenic and immunomodulatory potential).

Animal Model and Experimental Design

The experimental protocols were conducted at the Cantacuzino National Military-Medical Institute's Platform of Experimental Medicine, adhering to institutional and national ethical standards with approval from the Institute's Ethics Committee (authorization no: 15/17.05.2023). The study used 15 adult male Wistar rats from the Institute's

DOI : 10.62610/RJOR.2025.2.17.74

Specific Pathogen Free Animal Facility, which were maintained in a conventional housing system with controlled conditions (22-24°C, 40-60% humidity, and alternating 12-hour light/dark cycles) and provided unrestricted access to food and water. The study experimental design follows ARRIVE 2.0 guidelines, with daily veterinary supervision ensured throughout the study period.

The rats were assigned to three equal groups (n=5 per group). At study initiation, all subjects were weighed and anesthetized using a combination of Ketamine (0.5 mg/kg, Farmavet) and Medetomidine (0.5 mg/kg, Biotur). The procedure involved retro-orbital blood collection for biochemical and immunological analyses, followed by creation of bilateral femoral defects in the intercondylar space according to previously described methodology [31]. Bilateral femoral defects were created to maximize the experimental power while decreasing the required number of subjects, thereby increasing overall study efficiency. In order to improve experimental consistency, each rat received identical scaffold types (F1, F5, or F6) in both hind limbs, reducing the intra-individual variability factor. At the end of the surgical procedure, the effect of anesthesia was reversed using a small dose of Atipamezole (0.25 mg/kg, Biotur), and anti-inflammatory medication Ketoprofen (3 mg/kg, Dopharma) was administered for three consecutive days.

Hemolysis Testing

Before the surgical procedure, a preoperative blood sample was drawn via the retro-orbital route under anesthesia as an additional precautionary measure to evaluate the direct hemolytic potential of the composite biomaterials. Fresh venous blood was immediately incubated with scaffold fragments under standardized in vitro conditions. The testing protocol followed the ASTM F756-00 norms for evaluating the hemolytic properties of materials and was performed within the CI [27]. After an hour of incubation, samples were centrifuged, and the spectrophotometric assay measured the values of free hemoglobin released from lysed erythrocytes. The spectrophotometric readings were performed using a Jasco V-530 UV–VIS Spectrophotometer (Jasco, Tokyo, Japan), allowing high-sensitivity absorbance measurements. The results obtained ensured early screening of the hemocompatibility criteria before in vivo application.

Inflammatory and Osteogenic Serum Marker Analysis

Blood samples were taken at specific intervals—before surgery, and on Days 30 and 60 after implantation—using retro-orbital sinus puncture under anesthesia. All tests were carried out in the CI immunology lab, following Good Laboratory Practice (GLP) standards.

We used serum from blood samples to measure IL-6, IL-8, TNF-α, and IL-10 levels. The goal was to see the acute immune system's reaction after contact with the scaffolds. After hemostasis and coagulation, blood samples were centrifuged to separate the serum, which was then analyzed using the cytokine kit (R&D Systems Inc., Minneapolis, MN, USA) to determine the levels of IL-6, IL-8, TNF-α, and IL-10, assessing the immunological response (Rat Luminex Discovery Assay) immediately upon contact with the scaffolds.

DOI : 10.62610/RJOR.2025.2.17.74

Subsequent cytokine profiling was conducted on days 30 and 60 post-implantation. These longitudinal evaluations provided insight into the systemic inflammatory and immunoregulatory responses elicited by each scaffold formulation over time [32].

CRP levels were measured at Days 30 and 60 to evaluate systemic inflammation associated with each scaffold type. A Rat C-Reactive Protein (CRP) ELISA Kit (R&D Systems Inc., Minneapolis, MN, USA) was used to quantify CRP levels from serum samples, following the manufacturer's protocol. These measurements helped establish whether systemic inflammatory responses can be correlated with the localized immune modulation.

ALP levels were measured at Days 30 and 60 to evaluate the osteogenic potential associated with each scaffold type. A Rat Bone-Specific Alkaline Phosphatase (BALP) ELISA Kit (MyBioSource, USA, San Diego, California) was used to quantify ALP levels from serum samples, following the manufacturer's protocol. These measurements helped establish whether ALP levels observed in specific groups can be correlated with the bone regeneration processes.

To ensure that the experimental results had real biological meaning, the serum levels of certain inflammatory and osteogenic indicators were compared to the reference physiological ranges that have been described in the literature for adult male Wistar rats. These reference ranges were used as internal controls to help process the biochemical data collected after the surgical procedure.

For cytokine levels, literature data suggest baseline physiological serum concentrations: IL-6 below 50 pg/mL, TNF-α below 20 pg/mL, and IL-1β below 25 pg/mL. These values may vary depending on the assay type, experimental context, and physiological status of the animals, and can increase in the presence of systemic inflammation or tissue injury [22].

The normal range of CRP levels in healthy adult Wistar rats is 94–494 µg/mL, with an average level of about 341 µg/mL, based on ELISA quantification methods [32,33]. The normal physiologic range of ALP ranges between 70 and 300 U/L [34].

These reference values were used to interpret the progression of immunological and osteogenic responses in experimental animals at postoperative Days 30 and 60. Deviations from the normal were considered indicative of material-induced immunomodulation or bone regeneration dynamics, depending on the biomarker and direction of change.

Histopathological Analysis

Tissues were fixed in 10% neutral buffered formalin to keep the cells and matrix stable. Over the course of two weeks, Histo-Decal solution (Histo-Decal, Pantigliate, Italy) removed all of the calcium while keeping the tissue's shape. After they were processed, the samples were put in paraffin (Histopar, Remed ProdImpex, Bucharest, Romania), cut into 5 µm-thick slices, and stained with hematoxylin and eosin to look at their structure.

There were n = 6 histology samples in each scaffold group (3 animals × 2 femora) and the remaining 4 femoral pieces from each group were allocated for micro-CT imaging.

Digital slide scanning made it possible to see images in high detail and do further processing on them. The same specific

DOI : 10.62610/RJOR.2025.2.17.74

region of interest (ROI) was identified for all the slides at the level of the intercondylar defect. ImageJ allowed even better ROI visibility and made it simpler to see tissue characteristics. This made scoring far more accurate than just using standard microscopy.

The study looked at five histological signs of tissue regeneration: cell density, collagen matrix organization, mineralization level, vascularization, and inflammation.

Two experienced histopathologists independently examined and scored both the original scanned images and the improved ones processed in ImageJ. A semi-quantitative scoring system from 0 to 4 was used, where 0 indicated the absence of the feature and 4 represented the highest level observed.

When the evaluations of two people were more than one point apart, the evaluators looked at the images again and reached a final agreement on the score. Bilateral femoral samples from each animal were used to ensure the data could be compared between groups.

Statistical analysis

Because this preclinical investigation was exploratory and there were ethical limits on the number of experimental animals, a formal a priori power analysis was not done. The strategy followed the 3Rs approach, which means that it used as few animals as possible while still making sure that the results were consistent, strong, and could be validated across different types of imaging, even if there were fewer histological replicates [35].

Unless otherwise noted, all data are shown as mean ± SD. In each legend, the number of replicates (n) is shown.

Serological and Hemolysis Data Analysis

Serological markers (IL-6, IL-8, TNF-α, IL-10, CRP, ALP) and hemolytic activity (assessed according to ASTM F756-00) were analyzed using JASP software version 0.18.2 (University of Amsterdam, Netherlands), an open-source statistical tool suitable for both descriptive and inferential statistics. Data were imported in .csv format and processed using paired sample t-tests for temporal comparisons and repeated measures ANOVA for inter-group comparisons. Tukey's HSD post hoc test was used for pairwise group analysis. Statistical significance was considered at $p < 0.05$. Graphs depicting CRP and ALP evolution were generated using the integrated Plot.ly visualization tools. The use of JASP ensures transparency, replicability, and compliance with GLP norms for laboratory data processing.

Experimental Timeline Overview

The table below summarizes the full in vivo experimental timeline over the 60-day follow-up period. All animals were euthanized on Day 60. From each group (F1, F5, F6), three animals were processed for histological assessment. Other procedures, including imaging, blood sampling, and biocompatibility testing, were distributed across the timeline, as shown below in Table 1.

DOI : 10.62610/RJOR.2025.2.17.74

Table 1. Chronological Sequence of Experimental Procedures

Day	Procedure	Samples Involved	Purpose
Day 0	Surgical implantation of scaffolds (F1, F5, F6); baseline serology and *in vitro* hemolysis testing (ASTM F756-00)	All animals (n = 15)	Model initiation and baseline controls
Day 30	Blood collection for inflammatory and osteogenic markers	All animals	Mineralization status and systemic inflammation profiling
Day 60	Euthanasia	All animals;	Assessment of bone regeneration and scaffold integration
Day 60	Blood collection (CRP, ALP, IL-6, IL-10, TNF-α, IL-8)	All animals	Final systemic biomarker quantification
Day 60	Euthanasia and tissue collection; histological processing	3 animals/group	Evaluation of osteochondral regeneration at tissue level

Results

All graphical representations of serological outcomes (IL-6, IL-8, IL-10, TNF-α, CRP, and ALP) are directly derived from individual animal data, with group means, standard deviations (SD), and coefficients of variation (CV%) calculated transparently from raw values. This ensures internal consistency between tables, figures, and reported values, in line with ARRIVE guidelines and GLP-compliant reporting standards.

Hemocompatibility

The hemolytic properties of the selected scaffold formulations (F1, F5, and F6) were assessed using whole rat blood and conformed to the ASTM F756-00 standard. All three scaffolds presented hemolysis values well below the threshold of 5%, indicating excellent hemocompatibility (Figure 1).

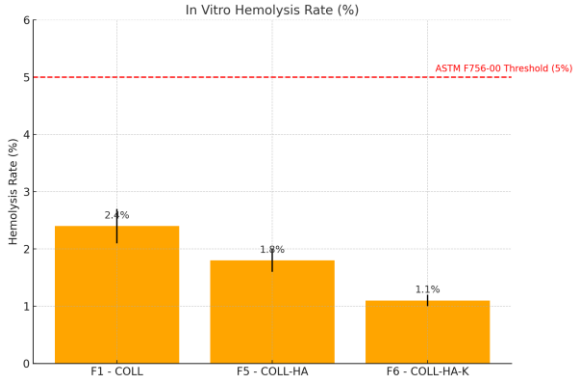

Figure 1. Hemolysis rate for scaffolds F1, F5, and F6 after 1h contact with rat blood

Cytokine profiles

The longitudinal analysis of cytokine profiles revealed dynamic shifts in systemic inflammatory and regulatory responses across different biomaterial formulations. Scaffolds incorporating hydroxyapatite and keratin (F6) were associated with a pronounced downregulation of pro-inflammatory cytokines such as IL-6, IL-8, and TNF-α when compared to collagen-only (F1) and collagen-hydroxyapatite (F5) scaffolds. The concurrent upregulation of IL-10 further highlights the immunomodulatory potential of keratin-enriched composites (Figure 2). The observed patterns at both intermediate (Day 30) and late (Day 60) time points indicate a stable anti-inflammatory environment related to the osteochondral regeneration (Figure 3 and Figure 4). The cytokine profile in the F6 group corresponds more closely with the histological data, bolstering the idea that immune modulation is a crucial factor in biomaterial efficacy.

DOI : 10.62610/RJOR.2025.2.17.74

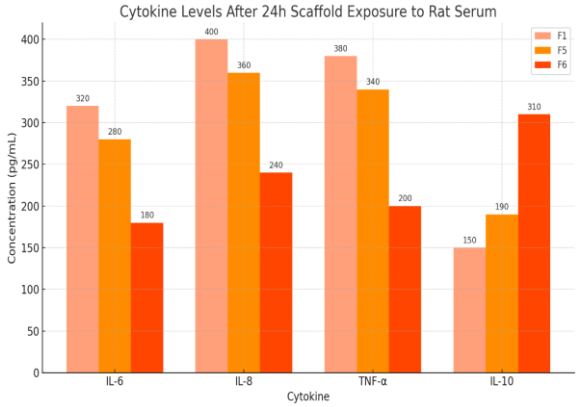

Figure 2. Cytokine profiles after 24h scaffold exposure, suggesting immunomodulatory advantage for F6.

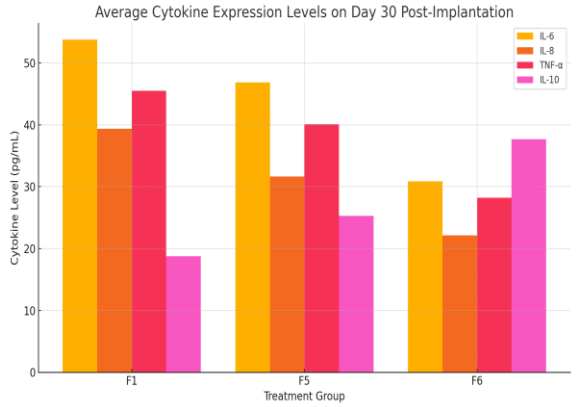

Figure 3. Cytokine expression levels in rat blood

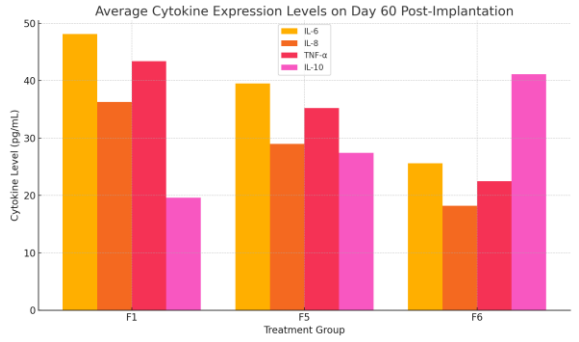

Figure 4. Cytokine expression levels in rat blood on Day 60 post-implantation

Post-implantation C-reactive protein (CRP) in the F6 group had decreasing values from 4.3 mg/L to 4.0 mg/L, a sign of a low-grade inflammatory state. This fact contrasts with the elevated CRP levels shown in the F1 and F5 groups, equivalent to a possible increased inflammation. The increase by +0.4 mg/L in the F5 group at Day 60 can be attributed to a delayed inflammatory reaction, due to the slower resorption of residual scaffold components. These findings illustrate the favorable cytokine and histological profiles of the F6 scaffold (Figure 5).

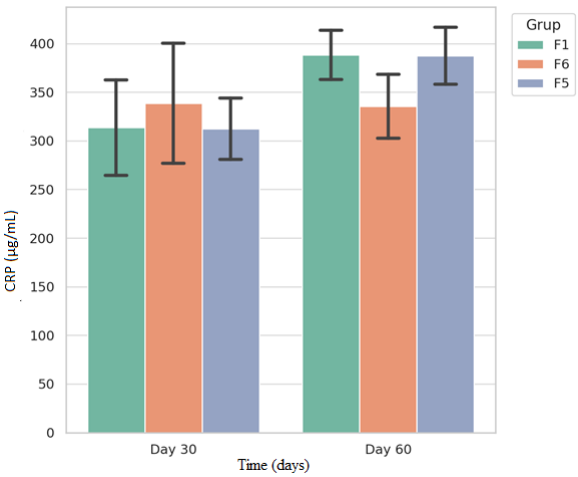

Figure 5. CRP level values during the experimental period

Serum alkaline phosphatase (ALP) levels reached the highest values in the F6 group, with a peak value of 72 U/L, indicating intense osteoblastic activity and possible ongoing bone remodeling. The F1 group manifested low ALP levels throughout the 60-day interval, and the F5 group showed only a moderate increase consistent with the osteoconductive influence of hydroxyapatite. The ALP response in the F6 group shows its predicted superior osteogenic potential, further supporting its efficacy in promoting new bone formation

DOI : 10.62610/RJOR.2025.2.17.74

in vivo (Figure 6).

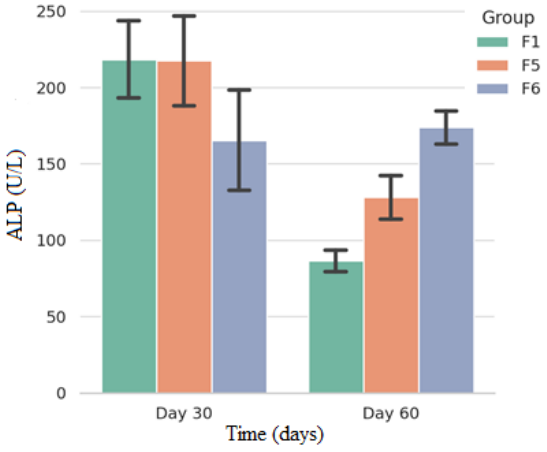

Figure 6. ALP level values during the experimental period.

Histological Assessment

The histopathological evaluation was conducted on specimens from only three animals per experimental group. To accommodate this limitation, the study design had to be adapted accordingly. Each animal received the same type of treatment at the level of the hind leg joints to maintain good intra-group consistency and allow correct interpretation across imaging, immunological, and histological data.

To compensate for the limitation of the reduced histological dataset, a descriptive and semi-quantitative approach was used, targeting the following criteria: cellularity, matrix organization, mineralization zones, and vascularization. The resulting slides were analyzed by two expert histopathologists, who formulated their conclusions using a scoring chart. The observations, in the form of the given score values, were compiled using weighted qualitative scoring, allowing meaningful data to be extracted.

Histological slides obtained revealed enhanced cellular infiltration, collagen matrix organization, and early mineral deposition in the F6 group. These histological outcomes confirm the regenerative profile of F6 (Table 3).

Table 3. Average Histological Scores per Scaffold Group (0–4 Scale)

Scaffold Type	Cell Density	Collagen Deposition	Mineralization	Vascularization	Residual Inflammation
F1 Coll	2.1	1.8	2.0	1.5	1.2
F5 Coll-HA	3.4	3.2	3.6	2.8	1.0
F6 Coll-HA-K	4.8	4.7	4.9	4.4	0.4

As illustrated in Figure 7, the total histological scores confirmed a progressive increase in regenerative performance from F1 to F6. The F6 scaffold showed the highest positive value, signifying enhanced efficacy in facilitating cellular infiltration, matrix formation, mineralization, and vascularization relative to the control and intermediate formulations.

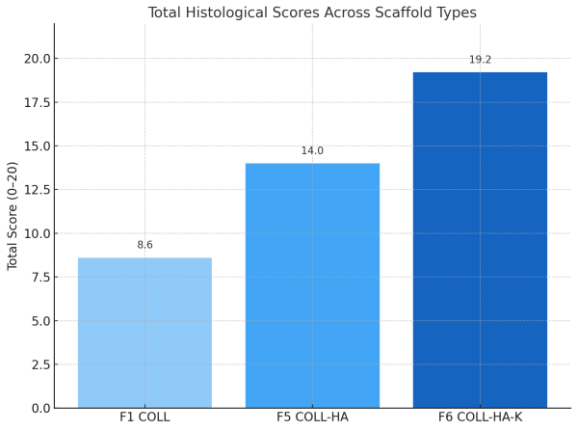

Figure 7. Total histological scores per scaffold group (F1, F5, and F6) were based on the sum of consensus values for five

DOI : 10.62610/RJOR.2025.2.17.74

parameters: cell density, collagen deposition, mineralization, vascularization, and residual inflammation. F5 and F6 have similar overall ratings, but F6 performs better on each specific criterion, especially in terms of matrix organization and vascularization. These results underscore the composite's favorable integration profile and regenerative consistency relative to the collagen-only group (F1).

The histopathological parameters are summarized in Table 4 and Figures 8-11.

Table 4. The characteristics of the histopathological parameters detected in the analyzed slides/group (F1, F5, and F6).

H.p/group	F1	F5	F6
Cell density	Moderate to high cell density is observed in the regeneration areas, with the presence of osteogenic cells: osteoblasts and mesenchymal cells	Significant, especially in the central areas of the image. There is an uneven distribution of cells, with areas of increased density in regions of active osteogenesis and around the forming bone trabeculae.	Increased, especially in regions of active regeneration and around the forming bone trabeculae. Peripheral areas show a lower cell density, characteristic of more mature bone tissue.
Collagen deposits	Moderate	Abundant, visible as fibrillar structures. The collagen matrix appears well-developed in some areas, indicating an advanced process of extracellular matrix formation.	Abundant. Fibrillar collagen structures are visible, especially in areas of active extracellular matrix formation. Collagen organization is observed in more mature structures at the periphery and is less organized in the central areas
Mineralized matrix	Present	Varying degrees, more developed in the region of the bone trabeculae	Present, especially at the periphery.
Vascularization	Several vascular structures are observed in the connective tissue, indicating a moderate degree of vascularization in the regeneration area	Rich, with numerous small blood vessels distributed throughout the tissue, especially in areas of active bone formation	Good, with multiple vascular structures distributed in the tissue
Residual inflammation	Moderate	Moderate	Moderate

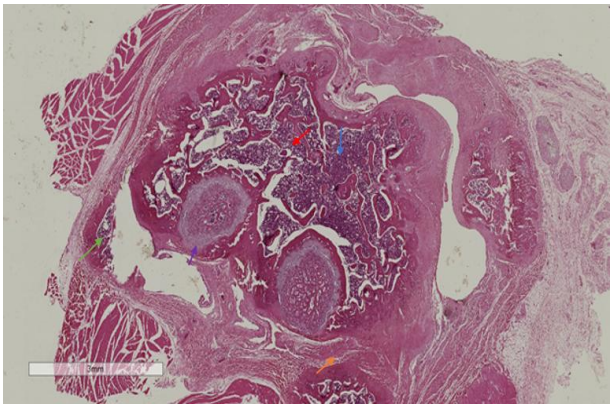

Figure 8. F1-COLL: Active osteogenesis process, with bone trabeculations and remodeling areas

DOI : 10.62610/RJOR.2025.2.17.74

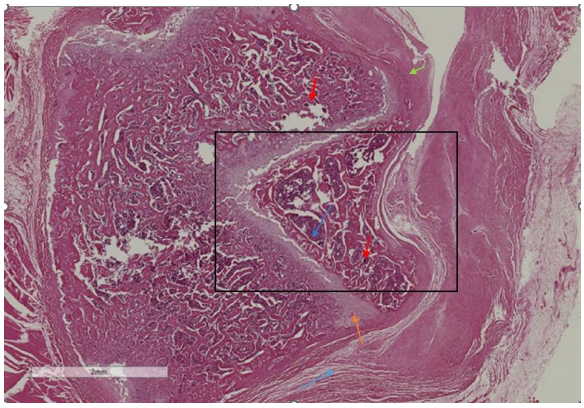

Figure 9. Formation of a complex trabecular network, with a pattern of interconnected bone trabeculae at different stages of maturation. This bony architecture shows the regeneration process. The central area illustrates signs of undergoing remodeling. New bone formation can be seen around the bone defect as well (black border). The 2mm scale indicates a significant bone defect in the healing process.

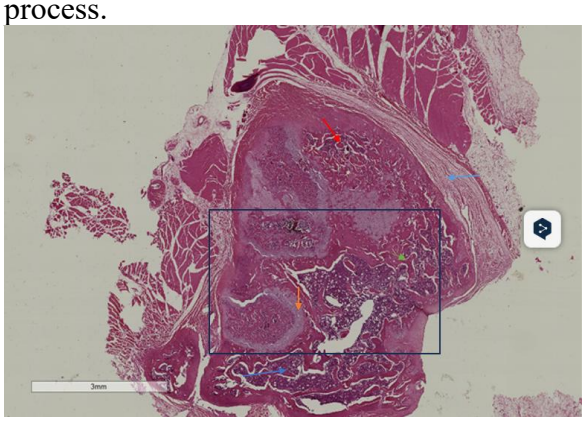

Figure 10. F6-COLL-HA-K: Bone defect undergoing regeneration, delimited by more mature bone margins. New bone trabeculae are forming in the center of the defect, with an irregular appearance characteristic of immature bone. Trabecular architecture is developing, with medullary spaces between the bone trabeculae (black border). This section shows an intermediate to advanced stage of the bone regeneration process, with significant new bone formation and ongoing remodeling.

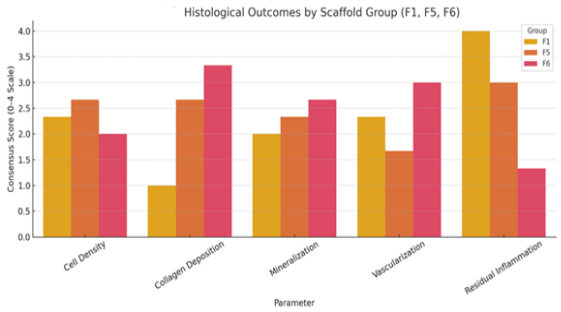

Figure 11. Consensus histological scores for each scaffold group at 12 weeks post-implantation. Bars represent the average consensus score for five semiquantitative histological parameters: cell density, collagen deposition, mineralization, vascularization, and residual inflammation.

Discussion

The findings of this study support the hypothesis that composite scaffolds integrating keratin and hydroxyapatite into a collagen matrix offer superior regenerative performance in osteochondral repair compared to simpler biocomposites. The F6 scaffold consistently outperformed the collagen-only (F1) and collagen-hydroxyapatite (F5) variants across all modalities evaluated, microstructural, immunological, and histological, demonstrating its ability to orchestrate a balanced osteoimmunological environment conducive to regeneration. These results are consistent with keratin's immunomodulatory [36] properties and hydroxyapatite's osteoconductive [37] properties.

Our results reinforce the fact that keratin-based materials have been shown to augment anti-inflammatory macrophage phenotype in vitro [38]. Hydroxyapatite contributes to bone mineralization and is a biocompatible support for cell adhesion and matrix deposition [9,39]. The synergistic behavior observed in F6 underscores the translational relevance of hybrid scaffolds that combine immunological and structural benefits.

DOI : 10.62610/RJOR.2025.2.17.74

Keratin is pivotal in modulating the immune response and the regenerative microenvironment. The F6 group showed an increase in IL-10 and a decrease in IL-6, TNF-α, and IL-8, in line with the characteristic of keratin-based materials to enhance M2 macrophage polarization, a form of immune reaction important in bone remodeling and inflammation response [38,40]. These immunological changes are critical, as sustained pro-inflammatory environments can delay bone healing.

The combination of collagen and hydroxyapatite provided an adequate osteoconductive scaffold for structural regeneration, as supported by literature sources [8,9,41], while the addition of keratin contributed to enhanced cell recruitment and angiogenesis, shown by the elevated histological scores. Keratin's involvement in the osteogenic differentiation of mesenchymal stem cells further supports its application in bone tissue engineering [13,16].

The keratin-containing scaffold promoted dense cellular infiltration, abundant collagen remodeling, and increased mineral deposition, suggesting that the interplay between scaffold composition and host response is determinant for effective regeneration. Combining ImageJ analysis and dual pathologist scoring increased reproducibility and analytical transparency, reducing potential bias and facilitating future replication.

The results suggest that keratin plays a more active role than previously expected, not only as a structural filler but also as a biologically active component capable of reshaping the local immune and regenerative environment.

Although the findings of this study are promising, several limitations can be mentioned.

The sample size was small from the start due to ethical concerns about using animals and the fact that the study was exploratory. Second, the study could only look at changes that happened within 60 days of the implant, so it couldn't look at long-term remodeling or possible scaffold resorption after that. To be sure that the reported regeneration effects last, future studies will need to use bigger groups of animals and longer observation periods. The major flaw of the current study is that it only uses young male Wistar rats. This method, preferred in preclinical research to limit hormonal variation, introduces possible flaws in the interpretation of results. Due to the fluctuating values of the circulating sex hormones in females, the estrogen and progesterone fluctuations significantly influence the bone metabolism [42, 43].

Female sex hormones significantly influence bone health by modulating the activity of osteoblasts and osteoclasts via distinct pathways compared to males [44]. Rats exhibit distinct sexual dimorphism, characterized by alterations in cytokine profiles and extracellular matrix metabolism [45]. Recent studies indicate that biomaterials exhibit varied interactions with host tissues, influenced by factors such as age, hormonal status, and sex of the subjects [46].

Although the results of this study are promising, they exclusively demonstrate the physiological responses of male subjects to the examined structures and cannot be directly generalized to female subjects. Future studies should equally include males and females to determine potential differences in osteochondral tissue healing and immune system responses.

The results of the present study open significant prospects for the clinical translation of biomimetic structures based on collagen-hydroxyapatite-keratin. The F6 formulation demonstrates superiority in vitro and in vivo tests and presents favorable commercial development and clinical implementation characteristics.

From a scalability perspective, the main components of the F6 material - collagen, hydroxyapatite, and keratin - are biomaterials with high availability and a

DOI : 10.62610/RJOR.2025.2.17.74

sustainable and easily accessible supply. Collagen can be easily obtained from bovine or porcine sources through standardized processes, hydroxyapatite can be obtained, and keratin can be extracted from renewable resources such as wool or poultry feathers, often considered waste in other industries and discarded [47,48]. This approach aligns well with the principles of the circular economy and reduces potential cost limitations to large-scale production.
This approach aligns well with the principles of the circular economy and reduces potential cost limitations to large-scale production.
The safety profile demonstrated by hemocompatibility tests and favorable immunological responses supports the potential for obtaining the regulatory approvals needed. The decreasing level of the pro-inflammatory cytokines and the rise of the anti-inflammatory cytokines diminish the likelihood of adverse reactions after implantation.
In the clinical context, these scaffolds could greatly impact the management of osteochondral defects, offering an alternative to autologous grafts (which involve donor site morbidity) or allografts (with risk of rejection and disease transmission). The F6 formulation can be customized for various orthopedic applications, from trauma to degenerative defects of bone and cartilage.
For effective translation to clinical use, additional studies in larger animal models are needed to investigate the performance of the scaffolds under adequate mechanical loading stress akin to the human bipedal model. Retail and Manufacturing Industry-academia collaborations and public-private sector partnerships could accelerate this process, facilitating a vectorial transition from basic research to end-line biomedical products available to patients.
More studies like the present one are valuable for further development in the field of tissue engineering and for the development of personalized regenerative medicine.

Conclusions

The results of this last in vivo study support the refinement and initial test confirmation of previously developed biomimetic scaffold formulations. The F6 scaffold demonstrated a reproducible profile of systemic safety, regenerative potential, and immunological stability in a validated bilateral osteochondral defect model.
All scaffold groups exhibited hemocompatibility based on ASTM F756-00 thresholds, confirming their safety upon blood contact. The cytokine profile in the F6 group corresponds more closely with the histological data, bolstering the idea that immune modulation is a crucial factor in biomaterial efficacy. The sustained downregulation of pro-inflammatory cytokines (IL-6, IL-8, TNF-α), consistently elevated IL-10 levels, and decreasing CRP concentrations in F6-treated animals confirm the establishment of a stable, low-inflammatory systemic profile. This immunological environment strongly supports regenerative processes, as evidenced by enhanced histological scores and increased ALP activity.
Although the findings of this study show a promising potential, we have found that a series of limitations can be identified.
The results of our present study are encouraging, but particular issues require consideration. The study animal lot was small from the beginning, and the in vivo research occurred within 60 days following implantation. Thus, it could not evaluate long-term remodeling or subsequent scaffold resorption.
. Future studies developed on larger animal groups with longer observation periods are necessary to confirm the results of this study.

The study's final results can be used to develop new types of keratin-enhanced

DOI : 10.62610/RJOR.2025.2.17.74

biomimetic scaffolds and medical devices, useful for the regenerative strategies in orthopedic surgery.

Funding: This research was funded by the internal project with the acronym LIZATE of the Cantacuzino National Military Medical Institute for Research and Development Bucharest, Romania, and is part of the own research for the doctoral thesis of Dr. Florin Popescu.

Conflicts of Interest: The authors declare no conflicts of interest.

References

1. Doukas WC, Hayda RA, Frisch HM, Andersen CRC, Mazurek CMT, Ficke CJR, et al. The Military Extremity Trauma Amputation/Limb Salvage (METALS) Study: Outcomes of Amputation Versus Limb Salvage Following Major Lower-Extremity Trauma. *J Bone Jt Surg-Am*, 2013 ;95(2):138–45.
2. Tintle SM, Forsberg JA. Extremity trauma: current concepts and advances. *J Am Acad Orthop Surg*., 2010;18(Suppl 1):10–9.
3. Cross WW, Swiontkowski MF. Treatment principles in the management of open fractures. *Indian J Orthop*., 2008 Oct;42(4):377–86.
4. Hosny GA, Ahmed ASAA. Neglected war injuries: Reconstruction versus amputation. *Injury*. 2023; 54(12):111085.
5. Mobasheri A, Batt M. An update on the pathophysiology of osteoarthritis. *Ann Phys Rehabil Med,* 2016; 59(5–6):333–9.
6. Gorbachova T, Amber I, Beckmann NM, Bennett DL, Chang EY, Davis L, et al. Nomenclature of Subchondral Nonneoplastic Bone Lesions. *Am J Roentgenol.,* 2019; 213(5):963–82.
7. Sanders TL, Pareek A, Obey MR, Johnson NR, Carey JL, Stuart MJ, et al. High Rate of Osteoarthritis After Osteochondritis Dissecans Fragment Excision Compared With Surgical Restoration at a Mean 16-Year Follow-up. *Am J Sports Med.*, 2017; 45(8):1799–805.
8. Dorozhkin S. Calcium Orthophosphate-Based Bioceramics. *Materials*., 2013; 6(9):3840–942.
9. Klenke FM, Liu Y, Yuan H, Hunziker EB, Siebenrock KA, Hofstetter W. Impact of scaffold architecture on the osteoconductivity of ceramic materials. *Tissue Eng Part A*., 2008;14(3):493–502.
10. Hwangbo H, Lee H, Roh EJ, Kim W, Joshi HP, Kwon SY, et al. Bone tissue engineering via application of a collagen/hydroxyapatite 4D-printed biomimetic scaffold for spinal fusion. *Appl Phys Rev*., 2021;8 (2):021403.
11. Nitti P, Kunjalukkal Padmanabhan S, Cortazzi S, Stanca E, Siculella L, Licciulli A, et al. Enhancing Bioactivity of Hydroxyapatite Scaffolds Using Fibrous Type I Collagen. Front Bioeng Biotechnol [Internet]. 2021 Feb 4 [cited 2024 Mar 30];9. Available from: https://www.frontiersin.org/articles/10.3389/fbioe.2021.631177
12. Chacon EL, Bertolo MRV, De Guzzi Plepis AM, Da Conceição Amaro Martins V, Dos Santos GR, Pinto CAL, et al. Collagen-chitosan-hydroxyapatite composite scaffolds for bone repair in ovariectomized rats. *Sci Rep*., 2023; 13(1):28.
13. Vermeulen S, Van Dyck M, Van Damme EJM. Keratin-based biomaterials: a review of protein chemistry and applications in regenerative medicine. *Mater Sci Eng C*., 2021;118:111478.
14. Vasconcelos A, Cavaco-Paulo A. The use of keratin in biomedical applications. *Curr Drug Targets*., 2013;14(5):612–9.
15. Wu AM, Bisignano C, James SL, Abady GG, Abedi A, Abu-Gharbieh E, et al. Global, regional, and national burden of bone fractures in 204 countries and territories, 1990–2019: a systematic analysis from the Global Burden of Disease Study 2019. *Lancet Healthy Longev*., 2021; 2(9):e580–92.

DOI : 10.62610/RJOR.2025.2.17.74

16. Lin YH, Huang KW, Chen SY, Cheng NC, Yu J. Keratin/chitosan UV-crosslinked composites promote the osteogenic differentiation of human adipose derived stem cells. *J Mater Chem B*., 2017; 5(24):4614–22.
17. Aadil KR, Bhange K, Kumar N, Mishra G. Keratin nanofibers in tissue engineering: bridging nature and innovation. *Biotechnol Sustain Mater*., 2024; 1(1):19.
18. Lee KH, Lee DW, Kang BC. The 'R' principles in laboratory animal experiments. *Lab Anim Res*., 2020; 36(1):45.
19. Arifin WN, Zahiruddin WM. Sample Size Calculation in Animal Studies Using Resource Equation Approach. *Malays J Med Sci MJMS*., 2017; 24(5):101–5.
20. Ito M. [Animal models for bone and joint disease. Assessment of bone mass, structure and strength in rat and mouse models - focus on micro-computed tomography study -]. *Clin Calcium*., 2011; 21(2):242–52.
21. McGovern JA, Griffin M, Hutmacher DW. Animal models for bone tissue engineering and modelling disease. *Dis Model Mech*., 2018; 11(4):dmm033084.
22. Giffen PS, Turton J, Andrews CM, Barrett P, Clarke CJ, Fung KW, et al. Markers of experimental acute inflammation in the Wistar Han rat with particular reference to haptoglobin and C-reactive protein. *Arch Toxicol*., 2003; 77(7):392–402.
23. Kraehenbuehl T, Ferreira JL, Hubbell PT. Bone regeneration and the Wistar rat model. *Eur Cell Mater*., 2008;15:50–60.
24. Zhang H, Bao R, Xu J, Ge Y, Chen Z, Fan M, et al. Development and Evaluation of a Rat Model of Full-Thickness Cartilage Defects. *J Vis Exp*. 2023; (195):64475.
25. Moran CJ, Ramesh A, Brama PAJ, O'Byrne JM, O'Brien FJ, Levingstone TJ. The benefits and limitations of animal models for translational research in cartilage repair. *J Exp Orthop*., 2016; 3(1):1.
26. Popescu F, Titorencu I, Albu Kaya M, Miculescu F, Tutuianu R, Coman AE, et al. Development of Innovative Biocomposites with Collagen, Keratin and Hydroxyapatite for Bone Tissue Engineering. *Biomimetics*., 2024; 9(7):428.
27. ASTM F756, Standard Practice for Assessment of Hemolytic Properties of Materials [Internet]. ASTM International; 2009 [cited 2025 Apr 27]. Available from: https://www.astm.org/f0756-17.html
28. Cameron ML, Fu FH, Paessler HH, Schneider M, Evans CH. Synovial fluid cytokine concentrations as possible prognostic indicators in the ACL-deficient knee. *Knee Surg Sports Traumatol Arthrosc*., 1994; 2(1):38–44.
29. Kapoor M, Martel-Pelletier J, Lajeunesse D, Pelletier JP, Fahmi H. Role of proinflammatory cytokines in the pathophysiology of osteoarthritis. *Nat Rev Rheumatol*., 2011;7(1):33–42.
30. Popescu F, Albu Kaya MG, Miculescu F, Coman AE, Ancuta DL, Coman C, et al. Novel Collagenous Sponge Composites for Osteochondral Regeneration in Rat Knee Models: A Comparative Study of Keratin, Hydroxyapatite, and Combined Treatments. *Cureus* [Internet]. 2024 Nov 11 [cited 2025 Apr 19]; Available from: https://www.cureus.com/articles/298247-novel-collagenous-sponge-composites-for-osteochondral-regeneration-in-rat-knee-models-a-comparative-study-of-keratin-hydroxyapatite-and-combined-treatments
31. Ancuta DL, Crivineanu M, Soare T, Coman C. In vivo effects of titanium implants treated with biomaterials in the bone regeneration process. *Vet Med J.,* 2021; 66:155–60.
32. Gautreaux MA, Tucker LJ, Person XJ, Zetterholm HK, Priddy LB. Review of immunological plasma markers for longitudinal analysis of inflammation and infection in rat models. *J Orthop Res*., 2022; 40(6):1251–62.
33. Zhou HH, Tang YL, Xu TH, Cheng B. C-reactive protein: structure, function, regulation, and role in clinical diseases. *Front Immunol*., 2024;15:1425168.
34. Owu DU, Osim EE, Ebong PE. Serum liver enzymes profile of Wistar rats following chronic consumption of fresh or oxidized palm oil diets. *Acta Trop*., 1998; 69(1):65–73.

DOI : 10.62610/RJOR.2025.2.17.74

35. Biau D, Kerneis S, Porcher R. Statistics in brief: the importance of sample size in the planning and interpretation of medical research. *Clin Orthop*., 2008; 466(9):2282–8.
36. Dias GJ, Ramesh N, Neilson L, Cornwall J, Kelly RJ, Anderson GM. The adaptive immune response to porous regenerated keratin as a bone graft substitute in an ovine model. *Int J Biol Macromol.,* 2020;165:100–6.
37. Dias GJ, Mahoney P, Hung NA, Sharma LA, Kalita P, Smith RA, et al. Osteoconduction in keratin-hydroxyapatite composite bone-graft substitutes. *J Biomed Mater Res B Appl Biomater*., 2017;105(7):2034–44.
38. Waters M, VandeVord P, Van Dyke M. Keratin biomaterials augment anti-inflammatory macrophage phenotype in vitro. *Acta Biomater*., 2018; 66:213–23.
39. LeGeros RZ. Calcium Phosphate-Based Osteoinductive Materials. *Chem Rev*., 2008;108(11):4742–53.
40. Fu Y, Yang W, Song Z, Wang C, Lu H. Keratin scaffolds with M2 macrophage polarization enhance skin wound healing. *Regen Biomater.*, 2021;8(4):rbab047.
41. Dorozhkin SV. Bioceramics of calcium orthophosphates. *Biomaterials*., 2010; 31(7):1465–85.
42. Hart D, Lamas JA, Trevisan C, et al. Sex differences in osteoarthritis pathogenesis: a comprehensive review. *Nat Rev Rheumatol*., 2022;18(10):593-608.
43. Melvin JS, Dombrowski AM, Torrance AG, et al. Sex-specific differences in stem cell mobilization and musculoskeletal regeneration. *Stem Cells Int.,* 2020; 2020:8192383.
44. Khosla S, Monroe DG. Regulation of bone metabolism by sex steroids. *Cold Spring Harb Perspect Med,.* 2018;8(1).
45. Klein SL, Flanagan KL. Sex differences in immune responses. *Nat Rev Immunol*., 2016;16(10):626-638.
46. Velasco-Mallorquí F, Rodríguez-Comas J, Ramón-Azcón J. Sex-specific differences in biomaterial-based tissue engineering strategies for regenerative medicine. *Biomaterials*., 2023; 295:122102.
47. Sharma S, Gupta A. Sustainable keratinous biomaterials: opportunities and challenges. *Curr Opin Green Sustain Chem*., 2021; 30:100477.
48. Sundaramurthi D, Krishnan UM, Sethuraman S. Sustainable keratin-based biomimetic scaffolds in tissue engineering applications. *Front Bioeng Biotechnol.,* 2022;10:935386.

DOI : 10.62610/RJOR.2025.2.17.74